MATERIALE PLASTICE
https://revmaterialeplastice.ro
https://doi.org/10.37358/Mat.Plast.1964

Influence of ZnO Nanomaterial Shape on UF Membrane Properties: a Comparative Study Between Nanoparticles And Nanowires

STEFAN CATALIN PINTILIE[1], LAURENTIA GEANINA PINTILIE[2*], STEFAN BALTA[2*], IULIAN GABRIEL BIRSAN[1]

[1]Dunarea de Jos University of Galati, Cross-border Faculty, Department of Applied Sciences, 47th Domneasca Str., 800008, Galati, Romania

[2]Dunarea de Jos University of Galati, Faculty of Engineering, Department of Environmental Engineering and Industrial Security, 47th Domneasca Str., 800008, Galati, Romania

Abstract: *Membrane research has managed to reach ever greater heights. The optimization of membrane processes is of common interest to industry, research and the domestic environment. Nanomaterials have been progressively researched in the membrane sector within the last decade, contributing in particular to their beneficial properties for the prevention of membrane fouling. This research investigates the effect of two shapes of ZnO nanomaterials, respectively nanoparticles and nanowires, on the properties of ultrafiltration membranes composed of 25 wt.% polysulfone. The method of membrane manufacturing is phase inversion, the immersion precipitation technique, and the procedure of nanomaterial incorporation into the polymeric matrix is known as blending. The results demonstrated the positive influence of nanomaterials on the performance of membranes, regardless of their shape, compared to the control membrane. In terms of permeability, the membrane with addition of ZnO nanoparticles showed an increase of 207.19 %, while the membrane with addition of zinc oxide nanowires recorded an increase of 89.16 %.*

Keywords*: ultrafiltration, nanocomposites, nanoparticles, nanowires, ZnO*

1. Introduction

During the last decade, nanocomposite membranes have generated appreciation in the development of membrane technology, which are usually comprised primarily of a polymeric matrix embedded with nanoparticles [1, 2]. Goh and his colleagues (2015) outlined in a concise manner that the incorporation of nanometric particles into a polymeric matrix will lead to the creation of a unique polymer-nanomaterial interface, attributable to their quantum size with a highly active surface. Therefore, this incorporation is leading to redesigning the fundamental properties of nanocomposites that benefit both the matrix and the filler [3].

Related to the progress of nanotechnology, a significant part of the research activity has been oriented to the use of diverse nanomaterials, predominantly inorganic, in membrane technology applications. With respect to membrane optimization used in separation and purification processes via blending methods, it is therefore necessary to take their shape into account. Nanomaterials, often termed nano-objects, are classified according to the number of dimensions (in the Cartesian coordinate system X, Y, Z) within nanometric domain less than 100 nm. Thus, we distinguish three basic shapes which represent the main classes of structural dimensionality: nanoparticles (3 dimensions in the nano-3D domain), nanofibers/ nanowires (2 dimensions in the nano-2D domain) and nanoplates (1 dimension in the nano-1D domain) [4].

Nanoparticles [5, 6] and single or multiple walled nanotubes [7, 8] are among the most commonly used nanomaterials in membrane technology. In recent years, interest in nanowires has increased [9, 10]. The selection of nanomaterial structure is a significant aspect in the membrane manufacture due to the specific characteristics provided by each form.

**email: stefan.balta@ugal.ro; geanina.pintilie@ugal.ro*

Nonetheless, the economic component, namely the total costs of the final membrane relative to the overall performance of the manufactured membranes, is a significant factor to consider.

During the study of the influence of nanomaterial shape on membrane properties, the authors chose to opt for the use of a single concentration, 0.5 wt. %, and two shapes of nanomaterials, zinc oxide nanowires and zinc oxide nanoparticles. The nanocomposite membranes were compared both with each other and with a control membrane (pristine).

The dimensions of these nanomaterials are similar, in that the predominant diameter of the nanoparticles (<50nm) is equal to the declared diameter of the nanowires (50 nm with the length of 300 nm). The objective of this study is to observe differences in the characteristics and properties of membranes after these nanomaterials have been incorporated into the polymeric matrix.

From our knowledge, the comparison between zinc oxide nanowires and zinc oxide nanoparticles, particularly regarding the shape influence on the general properties of polysulfone membranes and specifically the mechanical properties, has not yet been discussed.

2. Materials and methods

2.1. Materials

Polysulfone (PSf, $(C_{27}H_{22}O_4S)_n$, Mw ~ 35000) was used as the polymeric matrix of membranes. N-methylpyrrolidone (NMP, C_5H_9NO, reagent grade) acted as the solvent. The additives in this study were zinc oxide nanoparticles (ZnO NPs, <50 nm) and zinc oxide nanowires (ZnO NWs, 50 nm/ 300 nm), received in the form of nanopowders. These materials were purchased from Sigma Aldrich, USA. In order to provide membrane resistance to high working pressures, non-woven PP-PE support (Novatexx 2471, Freudenberg, Germany) was used.

2.2. Membrane manufacture by phase inversion method

In order for a membrane to be in the form of thin film, a polymeric solution is required. All membranes were manufactured by the phase inversion method, the immersion precipitation technique.

The polymeric solutions in this study were obtained by dissolving 25 wt.% PSf in NMP solvent under continuous stirring for 24 h. In the case of nanocomposite membranes, 0.5 wt.% zinc oxide nanopowder were first mixed in the NMP solution for one hour, followed by the normal procedure. After the polymer-solvent and polymer-solvent-nanomaterial mixtures were homogenized for 24 h, the polymeric solutions were cast in thin films. Prior to casting, the support layer was fixed on a glass sheet, and then wetted with NMP to prevent the polymer from clogging the non-woven support. After the excess solvent was removed, an amount of polymer solution was poured onto the moistened support layer. Thereafter, a thin-film polymer solution with a thickness of 250 μm was cast using a special knife. After a short time, the drawn thin film was immersed in a coagulation bath containing distilled water as a non-solvent. In this step, the phase inversion occurs, where the exchange between solvent and non-solvent results in a porous polymeric film, representing the final membrane. After 15 min, the phase inversion is complete and the membrane is transferred and stored in a container containing distilled water to ensure that the solvent residue is completely removed. The membrane codes, as well as details regarding the content of nanomaterials and their dimensions are presented in Table 1.

Table 1. The obtained membranes and the concentrations of nanomaterials added to the polymeric solution for the studies of this work

Membrane code	ZnO nanomaterials		
	Concentration [wt.%]	Shape	Dimensions* [nm]
M0	0	-	-
M1	0.5	Nanowires	D=50; L=300
M2	0.5	Nanoparticles	D=50

**D – diameter; L – length.*

2.3. Experimental procedures

The obtained membranes were characterized from a physical, structural, chemical and mechanical point of view by advanced methods of analysis. The top-view and cross-section membrane structures were analyzed using a scanning electron microscopy SEM (FEI Quanta 200, Thermo Fisher Scientific, USA). The chemical composition of membranes was analyzed by X-ray scattering (EDX) (EDAX coupled with the SEM microscope), as well as Raman spectroscopy (Raman-HR-TEC-785, StellarNet, USA). The hydrophilic character of the membrane surfaces was determined by the contact angle method using a goniometer (OCA 15EC, DataPhysics, USA). Topographic characterization of membranes was performed using AFM (EasyScan 2 atomic force microscopy, NanoSurf, Switzerland). Determination of membrane porosity was accomplished by gravimetric method [11].

In order to integrate the membranes in water treatment processes, the permeation properties were determined by studying permeability, relative flux and the retention capacity of Congo Red dye (10 ppm) solution, with the help of a Dead-End filtration cell (HP4750, Sterlitech, USA).

The distilled water flux J [$Lm^{-2}h^{-1}$] of the studied membranes was determined using the equation:

$$J=V/(S\cdot t), \quad (1)$$

where V is the volume of filtered water [L], S is the active surface of the membrane through which the filtered water passes [m^2] and t is the filtration time [h]. This equation is also valid in the case of the 10 ppm Congo Red solution filtration, flux noted with J_{CR}.

The membrane permeability, P_{DW} [$Lm^{-2}h^{-1}bar^{-1}$], was obtained by consecutive flux testing at increasing pressures from 10 to 20 bar. With these values the permeability can be determined using the equation:

$$P_{DW} = J/\Delta p = V/(S\cdot t\cdot \Delta p), \quad (2)$$

where Δp represents the pressure gradient [bar].

The membrane retention degree, R_{CR} [%], was determined by UV-Vis spectroscopic method (Hach DR5000, USA). The equation for determining the degree of retention is:

$$R_{CR} = [(C_i-C_f)/C_i]\cdot 100, \quad (3)$$

where C_i and C_f represent the initial concentrations, before filtering the dye solution, and final, after filtration [ppm].

The membrane fouling behavior during filtration of Congo Red solution can be determined by the relative flux method, Rel_{flux}, with the following equation:

$$Rel_{flux} = J_{CR}/J \quad (4)$$

The compaction degree, CD [%], was measured from the results of the distilled water flux. It shows the total loss of flux, expressed as percentage, by the ratio between the final value of the flux, J_f, and the initial value of the flux, J_i, by the following equation:

$$CD = [1-(J_f/J_i)]\cdot 100 \quad (5)$$

The determination of the total membrane performance was expressed in performance indices, which are dimensionless units. This index is determined using the data provided by a radar chart. Here, each membrane has a specific surface depending on the obtained performances (permeability, retention, relative flux reduction, modulus of elasticity and tensile strength), noted with S_{real}, these parameters being transformed into levels from 1 to 10, 10 representing the membrane that recorded the highest value for a

mentioned parameter. Also, an ideal surface, S_{ideal}, composed only of the maximum values recorded by all membranes, can be extracted from the radar chart. Knowing the values of the two types of surfaces, we can determine the performance index (PI) through the following equation:

$$PI = S_{real}/S_{ideal} \quad (6)$$

As the PI of the membrane tends towards 1, the membrane has many properties superior to the other studied membranes. As PI tends to 0, the properties obtained by the membrane are not desirable due to poor performance. As a justification note, integrating the fouling tendency is very important in establishing the membrane performance index, but it is difficult to quantify in a clear value. In this respect, the relative flux reduction, RFR [%], was chosen in the PI determination, but inversely (100-RFR), being calculated as the last value extracted from the results of the relative flux, according to the equation:

$$RFR = (J_{CR} / J) \cdot 100 \quad (7)$$

The mechanical properties of the manufactured membranes were measured with a mechanical testing instrument (Instron 8850, UK) by applying the ISO 527-3 standard [12]. All tensile tests were performed at a constant tensile speed of 5 mm min^{-1} until the membrane sample was broken at room temperature.

3. Results and discussions

3.1. Membrane analysis by SEM method

One of the roles of nanomaterials in the manufacture of porous membranes is the property of pore formation [10]. At the beginning of the phase inversion process, the exchange between solvent and non-solvent occurs in the vicinity of nanomaterials. As one can see from the surface SEM images, the nanocomposite membranes (Figure 1b, 1c) have a higher number of surface pores compared to the control membrane (Figure 1a).

However, there are obvious differences between the nanocomposite membranes, namely that the membrane with the addition of ZnO nanoparticles (Figure 1c) has a higher pore density than the nanowire blended membrane. This phenomenon is closely connected with the significant differences between the active surfaces of the two nanomaterials. Assuming that the declared dimensions of the nanomaterials are constant throughout the matrix, and the specific bulk density of the zinc oxide is 5.606 g cm^{-3}, the theoretically active surface of the nanomaterials can be calculated.

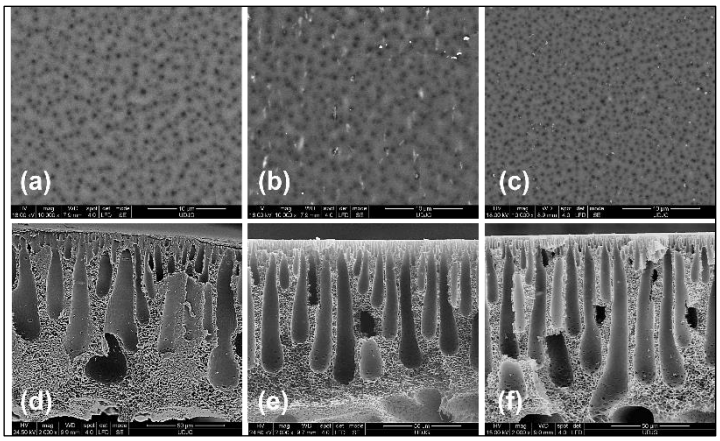

Figure 1. Top-view and cross-section SEM images of control membrane (a, d) and of membranes with ZnO nanowire (b, e) and ZnO nanoparticles (c, f)

Thus, perfectly spherical zinc oxide nanoparticles have a value of 21.41 $m^2 g^{-1}$, and perfectly cylindrical zinc oxide nanowires have an active surface of 15.46 $m^2 g^{-1}$. According to the dimensions of the two types of nanomaterials, where the diameter is similar and the length of the nanowires is six times the diameter of the nanoparticles, the active surface of the ZnO nanoparticles is theoretically greater by 38.46 % than the active surface of the nanowires. Numerous works have correlated the active surface with the pore-forming role of nanomaterials during the phase inversion of the membrane fabrication process [13].

By a larger surface of the nanoparticles we can also understand a much higher frequency of their number in the polymeric solution for membrane formation. Being larger in number to the same amount of nanomaterial in the polymeric solution and taking into account their hydrophilic character, the formation of a greater number of pores is certain for ZnO nanoparticles.

Normally, when no additives are present in the polymer solution (Figure 2.M0), at the beginning of phase inversion process, the water molecules from the coagulation bath will enter in a random/chaotic manner at the polymer solution-water interface, producing surface pores of variable size with random arrangement. This is consistent with the surface SEM image of the control membrane. Here, the phase inversion phenomenon is primarily dependent on coagulation bath temperature, which can create considerable differences in permeation properties [14].

In the case of nanocomposite polymeric solutions, as one can see in Figure 2 M1, M2, there is another important parameter, namely the presence of additives, particularly nanomaterials. Water molecules penetrate the polymer solution in a more orderly manner. Due to the nanoparticle's ubiquity, the path of the water molecules is always in their vicinity, leading to the appearance of an additional number of surface pores (Figure 2B.M2 and Figure 1c) of smaller dimensions, however more elongated and narrower structure macrovoids (Figure 2C.M2 and Figure 1f).

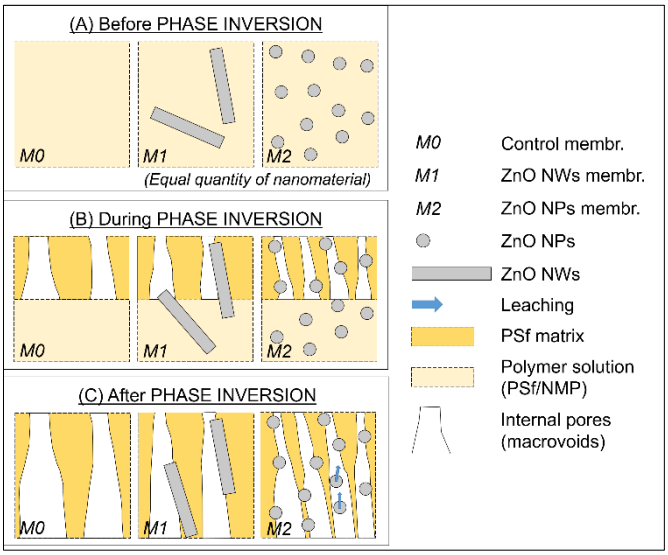

Figure 2. Schematic diagram regarding nanomaterial behavior in the polymeric solution during phase inversion

In the case of nanowires, no major changes in the size and ordering of pores can be seen on the membrane surface, being approximately identical with characteristics of control membrane (Figure 1b). Due to the lower number of nanowires, compared to nanoparticles, the ability to create surface pores is not as effective (Figure 2.M1). In contrast, the influence of nanowires on the formation of macrovoids is observable on the membrane's cross-section (Figure 1e), being more uniform.

Considering in particular the size of the nanomaterials, we can accept that nanoparticles have a more obvious imprint on the membrane structure compared to nanowires. Of course, there are disadvantages, namely that due to the overall smaller size, the possibility of nanoparticle detachment from the solution

(leaching) (Figure 2C) is unavoidable. Also, according to the literature, the incorporation of two-dimensional nanomaterials (i.e. nanowires) in the polymeric matrix of membranes minimizes the risk of leaching from the membrane matrix during filtration and assures a lower agglomeration tendency both on the surface and in the structure of the polymeric membranes [15].

In the SEM analysis of the cross-section structure (Figure 1), it is observed that the nanocomposite membranes have a different morphology from that of the control membrane (Figure 1d). In the case of the nanowire-blended membrane (Figure 1e), the macrovoids are finger-like, all having similar elongated structures, and the upper part does not have a visible connection with the lower area of the membrane, which can limit a high water flux. However, good organization of the resulting macrovoids can lead to increased mechanical properties.

The cross-sectional structure of the modified membranes by the addition of 0.5 wt.% ZnO nanoparticles (Figure 1f) has more and narrower macrovoids, which make the direct connection between the upper and lower area of the membrane. This type of structure facilitates the movement of water molecules through the membrane, which results in a high flux of water. The upper layer of the membrane, also called the active layer, is thinner, with denser pores compared to the control membrane. This is a defining aspect in the enhancement of the permeation properties.

3.2. EDX elemental analysis

According to the results provided by EDX in Table 2, the presence of nanoparticles on the membrane surface is twice as large compared to the membrane modified with ZnO nanowires.

Table 2. EDX elemental composition of the zinc detected in the membrane matrices

Membrane	Zinc [%]	
	Top-view	Cross-section
M0	-	-
M1	0.58 ± 0.14	0.31 ± 0.11
M2	0.77 ± 0.06	0.49 ± 0.07

Here it can be added that, due to the arrangement of the zinc element in the nanomaterial, the number of zinc atoms detected in the zinc oxide nanowires is smaller, because a large group of zinc atoms can be intercepted as a single atom. This is presumably due to a lower resolution of the EDX spectrometer.

This difference in concentration can also be explained by the fact that it is expected that the nanowires will be positioned upright (perpendicular to the membrane support) caused by the microfluxes occurring at phase inversion. In addition, the cylindrical shape favors the axial alignment in the direction of certain flows as opposed to the spherical shape.

Significant variation between the percentage values of zinc on the surface of the two membranes can be observed. In the case of nanoparticles, the detected concentration is almost 32 % higher.

The percentage of the zinc element in the section of the nanocomposite membrane with addition of nanowires is approximately equal to the mass percentage of 0.5 wt.% ZnO nanoparticles added to the polymeric solution.

3.3. RAMAN spectroscopy of membranes

Raman spectra were used to monitor the changes produced by the addition of nanomaterials to the membrane structure, in order to analyze the morphology of their constituents (Figure 3). The Raman wavenumbers characteristic to polysulfone spectral fingerprint can be identified, namely 640, 795, 1080, 1114, 1151 and 1591 cm^{-1}. Similar peaks have been observed by other authors [16- 20].

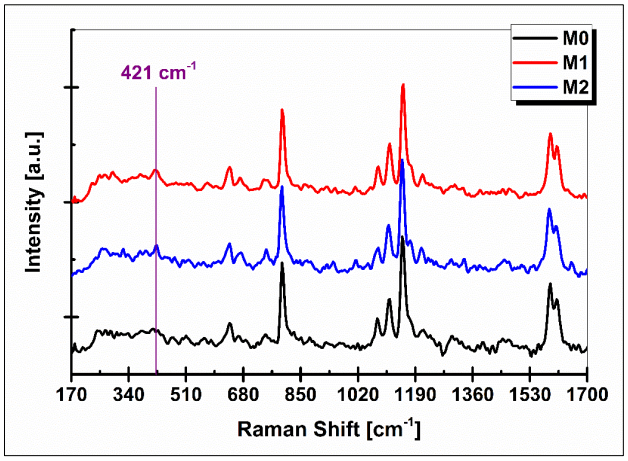

Figure 3. Raman spectra of membranes modified by the addition of zinc oxide nanoparticles and nanowires

The modification produced in the Raman spectra of the membranes after the incorporation of nanowires and nanoparticles is observed by a weak intensity at the Raman wavelength of 421 cm^{-1}. This peak is characteristic to zinc oxide and is found in the literature being defined as a characteristic peak of the würzite crystalline structure [21].

After Raman analysis, it can be confirmed that the crystalline structure of the two nanomaterials is mainly the same (würzite), and their presence in the nanocomposite membrane matrix is proved. Also, the structure of polysulfone did not undergo changes in the specific Raman domain after the addition of nanomaterials in polymeric solution, which means that both the nanoparticles and the nanowires did not alter the chemical structure of the polymer.

3.4. Hydrophilic character analysis by contact angle method

Due to the hydrophilic character of ZnO nanomaterials, it is observed in Table 4a that the contact angle of the nanocomposite membranes is smaller than that of the membrane without added nanoparticles (73.7°). Due to the blending of zinc oxide nanomaterials, the hydrophilic nature of the membranes decreases considerably for both the membranes modified by nanowires (59.7°) and for those with the addition of nanoparticles (56.6°). Similar trends were also observed by Al-Hinai et al [22].

Table 4. Contact angle (CA), porosity (ε), roughness (Sa), RFR, compaction factor (CF) and elastic modulus (Et) of the studied membranes

Membrane	Membrane parameters					
	(a) **CA [°]**	(b) **ε [%]**	(c) **S_a [nm]**	(d) **CF [%]**	(e) **RFR [%]**	(f) **E_t [MPa]***
M0	73.7±3.67	45±7.41	4.43±0.59	32.51±2.88	62.95±2.44	424.46±2.88
M1	59.7±9.08	49±9.21	4.78±0.56	1.26±0.35	50.51±1.29	735.22±49.58
M2	56.6±4.22	60±8.76	4.09±0.63	5.95±1.05	46.46±2.74	608.05±75.26

**Elastic modulus of the support layer is 358.80±46.54*

The hydrophilic character of the membranes is governed both by the surface chemistry, i.e. the presence of hydrophilic compounds, and by the surface roughness [23, 24]. These characteristics may explain the behavior of membranes during filtration as regards fouling.

3.5. Determination of membrane porosity

Characterizing the membrane's total porosity, shown in Table 4b, represents a method of asserting the types of structures observed in the surface SEM analyses (Figure 1 a, b, c) and in the cross-section (Figure 1 d, e, f).

Compared with the unmodified membrane, it can be observed that the incorporation of zinc oxide

nanowires in the polymeric solution led to a percentage increase of porosity of 8.89% while the incorporation of nanoparticles produced a percentage increase of 33.33%. These values confirm the discussion based on Figure 2.

3.6. Topographic characterization (AFM) of membranes

The membrane topography was analyzed by atomic force microscopy. 3D images of the analyzed surfaces (Figure 4) were obtained, enabling the presence of peaks and valleys to be observed. In the case of the control membrane (Figure 4A), a uniform relief is observed without major differences in peak structures, but with a higher apparent roughness. The incorporation of nanowires (Figure 4B) as well as of nanoparticles (Figure 4C) led to the emergence of prominent peaks of higher heights on the membrane surface.

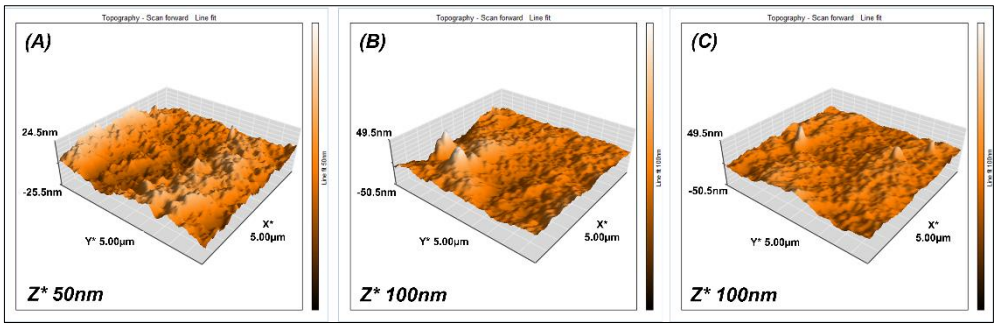

Figure 4. Three-dimensional representation by AFM method of the surfaces of control (A) and nanocomposite membranes with 0.5 wt% ZnO nanowire (B) and 0.5 wt% ZnO nanoparticle (C)

Table 4c shows the surface roughness values of the studied membranes. Although the presence of protrusions on the surface of membranes with addition of ZnO nanoparticles was observed, this did not increase the final roughness above the control membrane roughness value. Thus, in areas without these protrusions, the roughness of the nanoparticle membranes has a much lower roughness.

The decrease of surface roughness is explained by the nature of the nanoparticles in the polymeric solution to balance the transfer between solvent and non-solvent during the phase inversion, which leads to the formation of a uniform porous structure on the membrane surface [25], also observed in the surface SEM images (Figure 1c). A smoother surface usually leads to a lower contact angle.

On the other hand, the membranes with nanowires added have the highest roughness. However, due to the presence of the hydrophilic nanowires on the membrane surface, observed in the surface SEM images (Figure 1b), we can confirm the value of the contact angle is smaller than the control membrane (Table 4a).

3.7. Permeation tests

3.7.1. Membrane permeability

Figure 5 shows membrane permeabilities. These can provide information on the amount of filtered water, in which the values are reported as the total volume of filtered water through a square meter of membrane at a pressure of 1 bar.

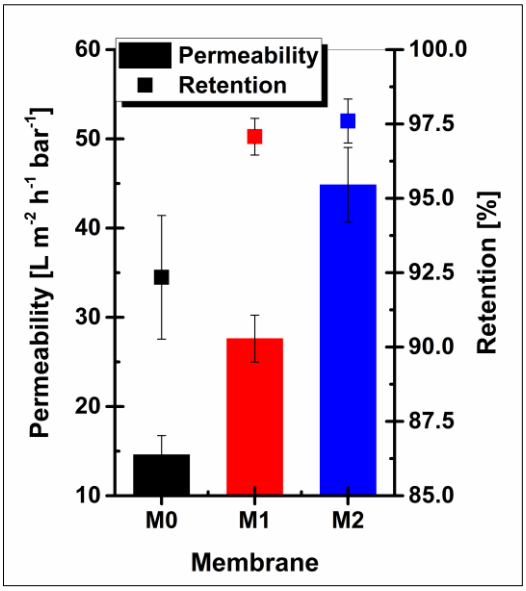

Figure 5. Permeability and retention degree of control and nanocomposite membranes

The lowest permeability is obtained by the control membrane, with a value of 14.6 $Lm^{-2}h^{-1}bar^{-1}$. The incorporation of zinc oxide nanowires produces a permeability increase of 89.16% higher, while nanoparticle-modified membranes exert an even higher permeability of 207.19% over the control membrane. The reason for the differences in the permeability increase is shown by the surface SEM micrographs (Figure 1), where a much larger number of pores is clearly observed in the case of zinc oxide nanoparticle blended membranes, while the nanowire membrane does not show an observable growth of the surface porosity.

Also, in many studies, the changes in flux and permeability were correlated with the differences in affinity for water, in which it was stated that an increase in hydrophilicity led to an increase in permeability [26, 27].

3.7.2. Retention degree of the studied membranes

The retention degree of Congo Red dye (Figure 5) increases with the addition of nanomaterials, the highest value being observed for the nanoparticle-blended membrane. The lowest retention capacity was obtained by the membrane without nanoparticles, with a value of 92.34%. Modification of membranes by addition of nanowires resulted in an increase of retention by 5.11% higher and in the case of membranes with ZnO nanoparticles an increase of the retention with 5.68% higher was observed, these being compared to the control membrane.

The retention capacity is closely related to the pore size on membrane surface [28]. This correlation is valid also for the membranes of this study, as the pore size decreases when there are nanomaterials (nanoparticles or nanowires) in the composition of the polymeric solution subjected to the phase inversion process. These results are confirmed by the surface SEM images of the control membranes and those modified with nanomaterials.

3.7.3. Compaction degree during filtration

Table 4d shows the compaction degrees for pure and nanocomposite membranes. These values were extracted from the results of pure water flux. As expected, the addition of zinc oxide nanowires in membrane matrix produced the lowest compaction degree during distilled water filtration. Incorporation of zinc oxide nanowires resulted in a 96% reduction in membrane compaction, while the addition of nanoparticles resulted in a decrease in compaction of 81.71%, percentages extracted from their comparison with the control membrane.

Possibly, in the absence of a proper mechanical test study, the compaction degree may convey some details on the mechanical behavior of the membranes. This method can be transposed/ translated, in mechanical terms, as a compression test of the polymeric film.

Alongside this, it is understood that this parameter is closely connected with the value of the modulus of elasticity of the membranes because its flexibility can decisively contribute to the compaction reduction after the efforts are applied perpendicular to the membrane (efforts arising from the increase of the pressure value, increase imposed by the separation process).

3.7.4. Study on the fouling degree of Congo Red dye (Relative Flux and Relative Flux Reduction)

The relative flux resulting from the relationship between the retention flux and distilled water flux, represents an important criterion in the study of the fouling phenomenon.

In Figure 6 it can be seen that the control membrane is more prone to fouling compared to the nanocomposite membranes. Due to the hydrophobic nature of the control membrane, it is easy to understand that during the filtration of Congo Red dye, the contaminant creates a dye-polymer hydrophobic bond.

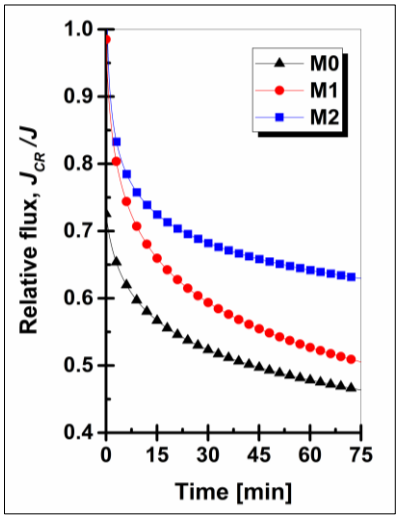

Figure 6. Relative fluxes of control and nanocomposite membranes modified with 0.5 wt.% zinc oxide nanowires and nanoparticles

The hydrophilicity increase of nanocomposite membranes, as well as the changes in roughness (Table 4c) led to the improvement of their fouling resistance. Due to the lower value of the contact angle and the most favorable roughness, the membrane modified with the addition of ZnO nanoparticles has the highest relative flux. From the stability point of view of the relative flux, it can be observed that the control membrane has not reached complete stabilization, while the nanocomposite membrane with addition of nanoparticles shows better stabilization towards the end of the filtration tests. This can be explained as an ability of nanoparticles on the membrane surface to induce detachments of contaminants deposited during filtration.

Even if the contact angle of the nanowire-blended membrane is smaller compared to the control membrane, the characteristic that in most cases is definitive in terms of fouling tendency, in this situation the relative flux of the nanowire-blended membrane is just as unstable as the control membrane, mainly due to the higher roughness of the membrane due to the addition of nanowires. Here, in contrast to the other type of nanocomposite membrane, contaminants are much easier to deposit in the membrane valleys due to the higher roughness value.

However, according to the RFR values in Table 4e, the relative flux reduction for the control membrane is the highest (62.95%), which means that fouling has occurred more. The addition of

nanowires results in a membrane with a difference in the relative flux reduction that, although it is not very large, nevertheless registered an RFR percentage decrease of 19.76%. It is clear that, with respect to the degree of fouling, the nanowires do not offer an obvious improvement to the membrane in the process of filtration of the Congo Red dye.

3.8. Mechanical properties of the studied membranes

3.8.1. Elongation-at-break and tensile strength

As it can be seen in Figure 7, the elongation-at-break of nanocomposite membranes resulted in an increase from 28.88% (control membrane) to 31.32%.

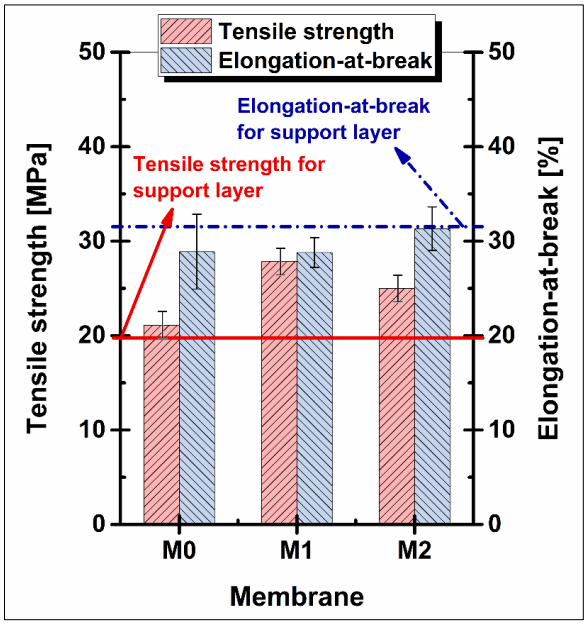

Figure 7. Elongation-at-break and tensile strength of the studied membranes and support layer. Standard deviation at elongation-at-break of the support layer: ± 1.258; Standard deviation of the tensile strength of the support layer: ± 1.789

Differences in size (especially length) between nanoparticles and nanowires are responsible for the distinct mechanical results of the formed membranes. The larger length of the nanowires provides greater links between the nanostructures and the polymer chains, which means that the energy transfer from the polymer to the nanowire is higher and the elongation is unchanged. In the case of nanoparticles, the membranes have a higher elongation, which means that they absorb the energy produced by mechanical stress, but at the same time produce a greater plastic deformation without breaking the sample.

The increase of tensile strength (Figure 7) for the membrane with addition of 0.5 wt% ZnO nanowires can be explained by the formation of a good stress transfer from the matrix to nanowires and, due to the high length of the nanowires (300 nm), they can lead at a more uniform stress distribution. This can minimize the occurrence of areas with high stress [29]. The optimum balance between tensile strength and elongation-at-break is achieved by the membrane with the addition of zinc oxide nanoparticles.

In addition, due to the fact that the studied membranes were cast and drawn on a non-woven support layer, the elongation-at-break and the tensile strength of the support layer were introduced in the figure. It can be observed that, even if the main purpose is to increase the mechanical strength of the membranes, the reported values of the support layer are quite different (depending on additive) than those of the final membranes. This aspect could confirm a close connection, especially physical, between the support layer and the cast polymeric solution.

3.8.2. Modulus of elasticity

Regarding the modulus of elasticity, the very good compatibility between nanowires and the polymeric matrix resulted in the formation of a membrane with the best mechanical properties.

As one can see in Table 4f, the highest value of the modulus of elasticity was confirmed for the membrane with the addition of 0.5 wt.% ZnO nanowire, with a percentage increase of 73.21% over the control membrane and a percentage value by 20.91% higher compared to the membrane with added zinc oxide nanoparticles. The explanation for this finding is similar to the case of elongation-at-break and tensile strength.

3.9. Determination of total membrane performance

For a better understanding of the efficiencies resulting from the modification of nanocomposite membranes with nanowires and nanoparticles, all the values resulting from various tests were transformed into levels from 1 to 10, where 10 represents the maximum performance obtained by a particular membrane.

By graphically displaying the total membrane performances, a clear tendency can be observed regarding the influence of zinc oxide nanomaterials (nanowires and nanoparticles) on the membranes. Figure 8 shows the most important performances of the membranes. It can be observed that for the permeation tests (Permeability, Retention and RFR), the nanoparticle-modified membrane has the best values, while the nanowire addition membranes have superior mechanical properties (Tensile strength and modulus of elasticity). The control membrane is presented by an irregular polygon of small area, denoting poor results after the evaluation of the main studied performances.

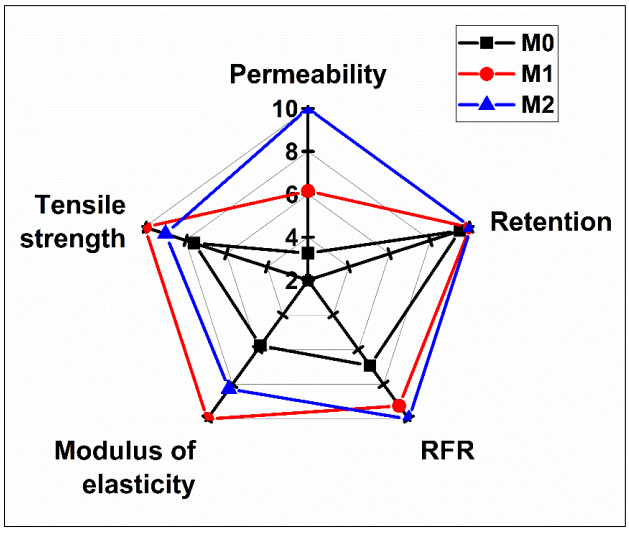

Figure 8. Performance chart of control membranes and those modified by addition of nanowires and nanoparticles

Table 5 presents the relationships between the real surfaces generated by the membrane performances and the ideal performance area.

Table 5. Performance index (PI) of control membranes and membranes modified by addition of zinc oxide nanomaterials

Membrane	PI
M0	0.41
M1	0.81
M2	0.89

The calculated indices confirmed that the addition of 0.5 wt.% ZnO nanoparticles in the polymeric solution produced the highest membrane performance, registering an increase of 117.07% over the pure membrane and 9.88% compared to the 0.5 wt% ZnO nanowire-blended membrane. The minor difference between the membrane with the addition of nanoparticles and the membrane with nanowires is determined primarily by the superior mechanical properties provided by nanowires to nanocomposite membranes. Due to the smaller size and the larger active surface, zinc oxide nanoparticles most positively influenced the general properties of the membranes.

4. Conclusions

In the study of the influence of the type of nanomaterial depending on form, the following conclusions are highlighted:

1. Addition of zinc oxide nanoparticles and nanowires in the polymeric solution led to an increase in surface porosity, the most pronounced being produced by nanoparticles. Evidence of these characteristics is confirmed by the high values of water flux and permeability, in which the nanoparticle-blended membrane showed a flux increase of 207.19% compared to the control membrane, and about 55% higher than the ZnO nanowire-modified membrane. These results are also confirmed by the calculated porosities, where porosity is directly proportional to the flux and permeability of distilled water.

2. The membrane retention degree increases due to the presence of nanomaterials in the membrane structure, the highest retention being of the membrane with the addition of nanoparticles.

3. Due to the hydrophilic character of zinc oxide nanomaterials, both types of nanocomposite membranes obtained a smaller contact angle which led to better fouling resistance properties compared to the control membrane. However, due to its superior hydrophilicity and smoother surface (lower roughness), the membrane with addition of zinc oxide nanoparticles obtained the best anti-fouling properties.

4. From the analysis of the tensile testing, it was found that the zinc oxide nanowires, used as a membrane modifying additive, offered them the best mechanical properties, with higher values compared to the control membranes and with the addition of nanoparticles.

5. The membrane with the best overall performance was the one with the addition of nanoparticles.

6. Due to the large interaction between nanoparticles and the polymeric matrix of the membrane, from the nanomaterial shape point of view we can conclude that the ideal choice, for the optimization of membrane processes, is by blending nanoparticles into the membrane structure.

References

1. RICHARDS, H.L., BAKER, P.G.L., IWUOHA, E., Metal Nanoparticle Modified Polysulfone Membranes for Use in Wastewater Treatment: A Critical Review, *Journal of Surface Engineered Materials and Advanced Technology*, **2**, 2012, 183-193.
2. URSINO, C., CASTRO-MUÑOZ, R., DRIOLI, E., GZARA, L., ALBEIRUTTY, M.H., FIGOLI, A., Progress of Nanocomposite Membranes for Water Treatment, *Membranes*, **8** (2), 2018.
3. GOH, P.S., NG, B.C., LAU, W.J., ISMAIL, A.F, Inorganic Nanomaterials in Polymeric Ultrafiltration Membranes for Water Treatment, *Separation & Purification Reviews*, **44** (3), 2015, 216-249.
4. ISO, ISO/TS 80004-2:2015(en), Nanotechnologies - Vocabulary - Part 2: Nano-objects.
5. BALTA, S., SOTTO, A., LUIS, P., BENEA, L., VAN DER BRUGGEN, B., KIM, J., A new outlook on membrane enhancement with nanoparticles: The alternative of ZnO, *Journal of Membrane Science*, **389**, 2012, 155-161.
6.JO, Y.J., CHOI, E.Y., KIM, S.W., KIM, C.K., Fabrication and characterization of a novel polyethersulfone/ aminated polyethersulfone ultrafiltration membrane assembled with zinc oxide nanoparticles, *Polymer*, **87**, 2016, 290-299.
7.TIRAFERRI, A., VECITIS, C.D., ELIMELECH, M., Covalent binding of single-walled carbon nanotubes to polyamide membranes for antimicrobial surface properties., *ACS Appl Mater Interfaces*, **3** (8), 2011, 2869-2877.

8.CHOI, J.H., JEGAL, J., KIM, W.N., Fabrication and characterization of multi-walled carbon nanotubes/polymer blend membranes, *Journal of Membrane Science*, **284** (1-2), 2006, 406-415.
9.WEI, Y., CHU, H.Q., DONG, B.Z., LI, X., XIA, S.J., QIANG, Z.M., Effect of TiO_2 nanowire addition on PVDF ultrafiltration membrane performance, *Desalination*, **272** (1-3), 2011, 90-97.
10. FENG, Y., LIU, Q., LIN, X., LIU, J.Z., WANG, H., Hydrophilic Nanowire Modified Polymer Ultrafiltration Membranes with High Water Flux, *ACS Applied Materials & Interfaces*, **6** (21), 2014, 19161–19167.
11. PINTILIE, S.C., TIRON, L.G., LAZAR, A.L., VLAD, M., BIRSAN, I.G., BALTA, S., The influence of ZnO/ TiO_2 nanohybrid blending on the ultrafiltration polysulfone membranes, *Mater. Plast.*, **55**(1), 2018, 54-62.
12. *** ISO, ISO 527-3:2018, Plastics - Determination of tensile properties - Part 3: Test conditions for films and sheets.
13.YULIWATI, E., ISMAIL, A.F., Effect of additives concentration on the surface properties and performance of PVDF ultrafiltration membranes for refinery produced wastewater treatment, *Desalination*, **273** (1), 2011, 226-234.
14.TIRON, L.G., PINTILIE, S.C., VLAD, M., BIRSAN, I.G., BALTA, S., Characterization of Polysulfone Membranes Prepared with Thermally Induced Phase Separation Technique, *IOP Conf. Series: Materials Science and Engineering*, **209**, 2017, 012013.
15. XU, Z., YE, S., FAN, Z., REN, F., GAO, C., LI, Q., LI, G., ZHANG, G., Preparation of Cu2O nanowire-blended polysulfone ultrafiltration membrane with improved stability and antimicrobial activity, *Journal of Nanoparticle Research*, (10) 2015.
16. KUVAREGA, A.T., KHUMALO, N., DLAMINI, D., MAMBA, B.B., Polysulfone/N, Pd co-doped TiO_2 composite membranes for photocatalytic dye degradation, *Separation and Purification Technology*, **191**, 2018, 122-133.
17. SHILTON, S.J., PROKHOROV, K.A., GORDEYEV, S.A., NIKOLAEVA, G. YU., DUNKIN, I.R., SMITH, W.E., PASHININ, P.P., Raman spectroscopic evaluation of molecular orientation in polysulfone, *Laser Physics Letters*, **1** (7), 2004, 336-339.
18. KIBECHU, R.W., NDINTEH, D.T., MSAGATI, T.A.M., MAMBA, B.B., SAMPATH, S., Effect of incorporating graphene oxide and surface imprinting on polysulfone membranes on flux, hydrophilicity and rejection of salt and polycyclic aromatic hydrocarbons from water, *Physics and Chemistry of the Earth, Parts A/B/C*, **100**, 2017, 126-134.
19.VICO, S., PALYS, B., BUES-HERMAN, C., Hydration of a Polysulfone Anion-Exchange Membrane Studied by Vibrational Spectroscopy, *Langmuir*, **19** (8), 2003, 3282-3287.
20. KIM, H.J., FOUDA, A.E., JONASSON, K., In situ study on kinetic behavior during asymmetric membrane formation via phase inversion process using Raman spectroscopy, *Journal of Applied Polymer Science*, **75** (1), 2000, 135-141.
21.LO, S.S., HUANG, D., Morphological Variation and Raman Spectroscopy of ZnO Hollow Microspheres Prepared by a Chemical Colloidal Process, *Langmuir*, **26** (9), 2010, 6762-6766.
22. AL-HINAI, M.H., SATHE, P., AL-ABRI, M.Z., DOBRETSOV, S., AL-HINAI, A.T., DUTTA, J., Antimicrobial Activity Enhancement of Poly(ether sulfone) Membranes by in Situ Growth of ZnO Nanorods, *ACS Omega*, **2** (7), 2017, 3157-3167.
23.LI, J.F., XU, Z.L., YANG, H., YU, L.Y., LIU, M., Effect of TiO_2 nanoparticles on the surface morphology and performance of microporous PES membrane, *Applied Surface Science*, **255**, 2009, 4725-4732.
24. RAZMJOU, A., RESOSUDARMO, A., HOLMES, R.L., LI, H., MANSOURI, J., CHEN, V., The effect of modified TiO_2 nanoparticles on the polyethersulfone ultrafiltration hollow fiber membranes, *Desalination*, **287**, 2012, 271-280.
25.YOGARATHINAM, L.T., GANGASALAM, A., ISMAIL, A.F., ARUMUGAM, S., NARAYANAN, A., Concentration of whey protein from cheese whey effluent using ultrafiltration by combination of hydrophilic metal oxides and hydrophobic polymer, *Journal of Chemical Technology*

and Biotechnology, **93** (9), 2018, 2576-2591.
26. HAMID, N.A.A., ISMAIL, A.F., MATSUURA, T., ZULARISAM, A.W., LAU, W.J., YULIWATI, E., ABDULLAH, M.S., Morphological and separation performance study of polysulfone/titanium dioxide (PSF/TiO_2) ultrafiltration membranes for humic acid removal, *Desalination*, **273**, 2011, 85-92.
27. CAO, X., MA, J., SHI, X., REN, Z., Effect of TiO_2 nanoparticle size on the performance of PVDF membrane, *Applied Surface Science*, **253** (4), 2006, 2003-2010.
28. HARUN, Z., JAMALLUDIN, M.R., YUNOS, M.Z., SHOHUR, M.F., ISMAIL, A.F., The Effect of Amorphous Rice Husk Silica to the Polysulfone Membrane Separation Process, *Advanced Materials Research*, **701**, 2013, 319-322.
29. ALAM, J., SHUKLA, A.K., ALHOUSAN, M., DASS, L.A., MUTHUMAREESWARAN, M.R., KHAN, A., AHMED ALI, F.A., Graphene oxide, an effective nanoadditive for a development of hollow fiber nanocomposite membrane with antifouling properties, *Advances in Polymer Technology*, 2017.

Manuscript received: 24.08.2020